Opt Quant Electron (2008) 40:1219–1225
DOI 10.1007/s11082-009-9305-2

High speed intracavity-contacted vertical cavity surface emitting lasers with separated quantum wells

V. V. Lysak · I. M. Safonov · Y. M. Song · I. A. Sukhoivanov · Yong Tak Lee

Received: 18 September 2008 / Accepted: 21 April 2009 / Published online: 20 May 2009

Abstract In this work, the simulation of the 980 nm InGaAs intra-cavity-contacted oxide-confined vertical-cavity surface-emitting lasers (ICOC VCSELs) with separated triplets of quantum wells (STQW) is presented. We analyze the thermal, electrical and optical properties of such devices. Results of simulations show the larger optical power efficiency and higher modulation bandwidth for devices with included STQW.

Keywords DC characteristics · Intracavity-contacted oxide-confined vertical-cavity surface-emitting laser · Modulation bandwidth

1 Introduction

Vertical-cavity surface-emitting lasers (VCSEL's) have bandwidths greater than 10 GHz and they are expected to play a key role for next-generation network transceivers (Krishnamoorthy et al. 2000). Over short distances inside computer systems or clusters of electronic networks, board-to-board or chip-to-chip multi gigahertz bandwidth optical interconnects are required to replace electrical interconnects. The optical interconnects include direct interconnects among boards, arbitrary interconnection patterns, channel isolation, and increased bandwidth, thus, avoiding the interconnection bandwidth bottleneck of systems with strictly in-plane electronic interconnects. Optical interconnects can be used in an increasing number of applications related to high data rate real time operations such as short distance networks, signal processing boards, etc. (Chu et al. 2004).

V. V. Lysak (✉) · Y. M. Song · Y. T. Lee
Department of Information and Communications, Gwangju Institute of Science and Technology, 1, Oryong-dong, Buk-ku, Gwangju 500-712, Republic of Korea
e-mail: lysak@gist.ac.kr

V. V. Lysak · I. M. Safonov
Kharkov National University of Radio Electronics, 14, Lenin ave, 61166 Kharkov, Ukraine

I. A. Sukhoivanov
Departamento de Electronica, FIMEE, Universidad de Guanajuato, Guanajuato, Mexico

VCSELs can be divided into two contacting schemes: extracavity - (EC) and intracavity - contacted (IC) structures. In the extracavity case, the carrier is injected into the active region by passing through the Distributed Bragg Reflector (DBR) mirror stack. In order to reduce the driving voltage and improve their power conversion efficiency the DBR resistance is decreased by grading the interfaces and making complex doping profiles that increase the optical losses (Lear and Chalmers 1993). In the intracavity-contacted oxide-confined VCSELs (ICOC-VCSELs) the active region is bordered by two highly doped contact layers to inject current. In this case, the current bypasses the substrate and both DBRs and hence the undoped mirrors without graded interfaces or dielectric mirrors, which minimize the optical losses, can be made (Scott et al. 1994).

In conventional EC VCSELs, the current travels about 3 μm vertically, and through the many heterointerfaces. This allows effective current spreading. However, in the ICOC VCSELs, the current flows in the horizontal direction because of the thinner contact layer, and there is not enough room for uniform carrier redistribution into the active layer as it travels through the spacer layers. Thus, it leads to a heavy current crowding at the rim of the oxide window resulting in higher optical losses and lower modulation bandwidth (Krishnamoorthy et al. 2000). To suppress the current crowding effect, the thickness of graded layer (GLT) at contact layer-oxide window aperture interface is optimized (Lysak et al. 2005)

To provide effective interaction of the laser mode with the gain medium, quantum wells can be separated, placing them in the antinodes of the mode profile (Raja et al. 1988). It allows increasing the number of QWs in the active layer of VCSEL. This structure was investigated experimentally (Kim et al. 1999), but there is no advanced theoretical models to provide more detailed information about the active layer structure and high speed characteristics for such structure.

In this work, we compare the simulation models with and without SQW and show that advanced structure can improve the power and modulation characteristics.

2 Structure description

The schematic representation of the simulated 980 nm ICOC VCSEL is presented in Fig. 1.

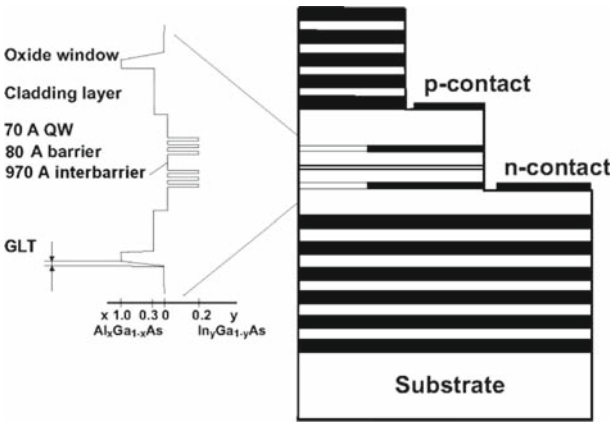

Fig. 1 Intracavity-contacted oxide-confined (ICOC) VCSEL structure with separated QWs

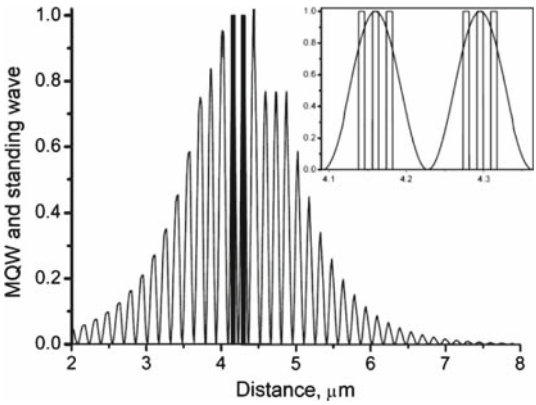

Fig. 2 The standing optical wave of the fundamental mode for structure with separated QWs

The active layer contains a pair of three 70/80Å $In_{0.2}Ga_{0.8}As$/GaAs QWs/barriers, separated by the inter-barrier designed to place a QWs in a maxima of generated field (see Fig. 2). Material for interbarrier layer is the same as barrier layer. The resonator contains two $Al_{0.3}Ga_{0.7}As$ cladding layers.

Oxide windows next to the quantum-well active region are formed by the lateral selective steam oxidation of AlAs to guide the current (to funnel current spreading from annular contact into the central active region), as well as the optical mode (to confine an optical field in radial direction) through the central region of the resonator (Sarzala 2004).

The 80 Å graded layer is placed at the contact layer-oxide window aperture interface for both p- and n-contacts to suppress the current crowding effect (Lysak et al. 2005). The width of the p- and n-contacts is 10 μm. The diameter of oxide window aperture is 14 μm and the diameter of top DBR is 20 μm. The top and bottom Bragg reflector stacks consist of 25 $Al_{0.9}Ga_{0.1}As$/GaAs and 27 AlAs/GaAs layer pairs, respectively. While p- and n-contact layers are parts of Bragg mirrors, the thickness of ones is $7\lambda/4n$ and $5\lambda/4n$, respectively (Lysak et al. 2006). Here λ is the operation wavelength, n is the refractive index of layer. The thickness of cladding and interbarrier layers are chosen to have the same operation wavelength for all structures.

3 Numerical simulations and description of results

The theoretical model of IC VCSEL including the optical, thermal and electrical properties was analyzed in (Scott et al. 1993). But in this model the main effects like temperature effect, spatial hole burning and optical field distribution are considered by simple analytical formulations. Additionally the n-contact layer was treated as a ground plain that did not fully describe the current flowing. In our case the self-consistent modeling of electrical, optical and thermal properties is used (PICS3D 2002). This model simulates wide spectrum characteristics with very large updating possibilities of new material parameters and calculation algorithms. Carrier transport is simulated using the drift-diffusion model. Calculations of the optical gain, refractive index and spontaneous recombination as a function of wavelength are based on $4 \times 4\vec{k} \cdot \vec{\mathbf{p}}$ band structure computations for the strained quantum wells.

The heat flux equation is included to address self-heating effects. Because of the multilayered VCSEL structure, the anisotropy of the thermal conductivity (Sarzala et al. 1996) and its temperature and composition dependence (Nakwaski 1988) are taken into account. All

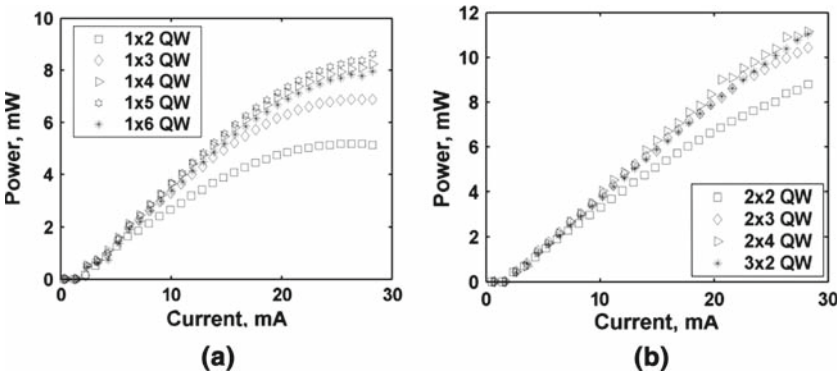

Fig. 3 L–I characteristics for VCSEL with different numbers of QWs

Table 1 Axial confinement factor for different VCSEL structures

1 × 2 QW	1 × 4 QW	1 × 6 QW	2 × 2 QW	2 × 3 QW	2 × 4 QW	3 × 2 QW
1.99	1.6	1.2	1.993	1.84	1.665	1.997

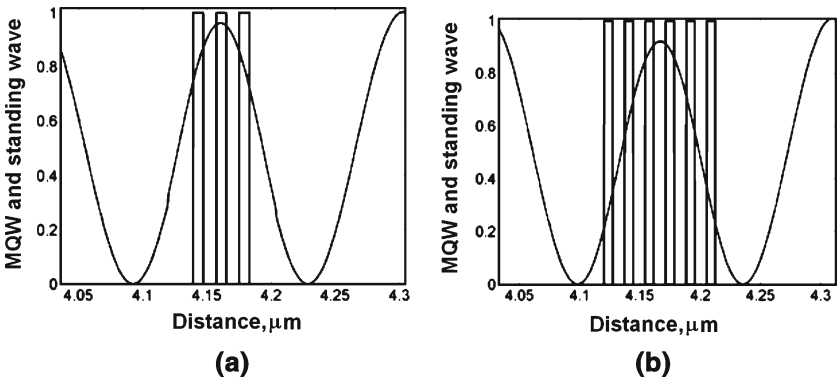

Fig. 4 The standing optical wave of the fundamental mode for structure with **a** 3 and **b** 6 QWs

important heat sources, i.e. nonradiative recombination, absorption of spontaneous radiation as well as volume and Joule heating, are taken into account (Wachutka 1990). The enhanced effective index method (Hadley et al. 1991) is employed for optical simulation including temperature effects on layer thickness, absorption, and refractive index. The lateral optical modes are given by Bessel functions. The main material parameters can be found in literature (Piprek 2003).

Figure 3 shows a light–current (L–I) characteristics for standard structure (Fig. 3a) and structure with periodic gain medium (Fig. 3b).

Figure 3a shows increasing the slope efficiency with increasing the numbers from 2 up 5 QWs, but than structure has 6 QWs, efficiency is decreased. It can be explained by decreasing of axial confinement factor (Wilmsen et al. 1999) (see Table 1).

The optical field for 3 and 6 QWs is presented in Fig. 4.

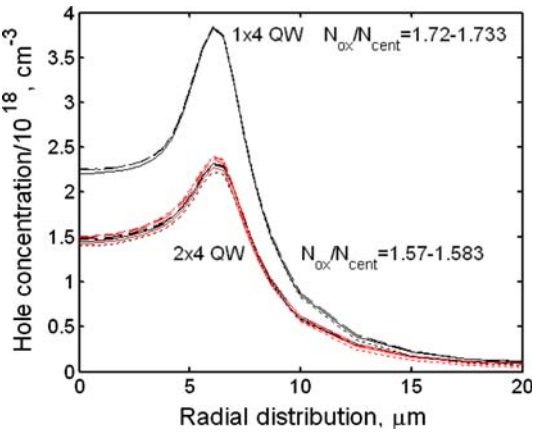

Fig. 5 Radial distribution of hole concentration in 1 × 4 and 2 × 4 QW devices

The slope efficiency for structures with periodic gain medium (Fig. 3b) with 2 × 3 QWs and 3 × 2 QWs is almost the same at small current value due to same number of QWs and axial enhancement factor. But at large pump current power is larger for 3 × 2 QWs device due to larger resonator length.

More efficient using of QW area gives us larger slope efficiency of L–I characteristics output power show the larger slope efficiency and maximal for device with periodic gain medium.

Other reason to increase the slope efficiency for laser with periodic gain medium is reduced current crowding. Figure 5 shows radial distribution of hole concentrations in 1 × 4 and 2 × 4 QW devices.

It is seen the ratio between the concentration under oxide window N_{ox} and in the center of device N_{cent} is lower for device with separated QWs.

4 Modulation response

The modulation properties of VCSEL can be predicted by the relaxation resonance. For bias currents sufficiently far above threshold to ensure effective carrier clamping, the frequency of this resonance is given by (Wilmsen et al. 1999):

$$f_R = \frac{1}{2\pi}\sqrt{\eta_i \frac{\Gamma \xi v_g}{q V_{eff}} \frac{\partial g}{\partial N}\,(I - I_{th})}, \tag{1}$$

where η_i is the internal quantum efficiency; Γ is the confinement factor; ξ is the energy confinement factor or gain enhancement factor; q is the electron charge; V_{eff} is the effective volume of resonator including the penetration depth of DBRs; $\partial g/\partial N$ is the differential gain; I is the bias current, and I_{th} is the threshold current.

Figure 6 shows the simulated 3-dB frequency dependence of the device on $\sqrt{I - I_{th}}$ for different structures.

The modulation conversion efficiency factors (MCEF) for different structures are presented in Table 2.

Table 2 shows the maximum MCEF for structure with 2 × 4 QWs at value of 242.1 GHz/(A)$^{0.5}$. Table also shows decreasing the MCEF for 3 × 2 QW structure due to larger volume of resonator with two interbarrier layers.

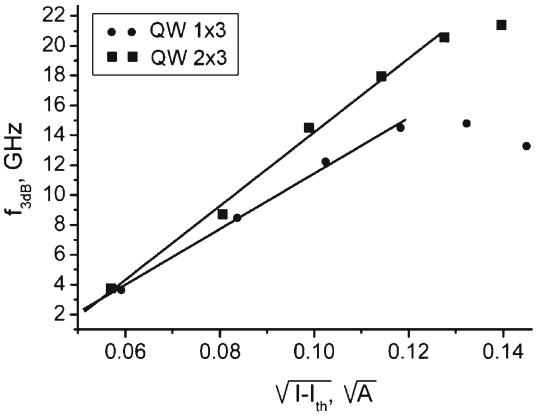

Fig. 6 The modulation conversion efficiency factor of VCSEL with different numbers of QWs

Table 2 MCEF value in GHz/(A)$^{0.5}$ for different structures

	1 × 2 QW	1 × 5 QW	1 × 6 QW	2 × 2 QW	2 × 3 QW	2 × 4 QW	3 × 2 QW
MCEF	72.5	117.3	102.1	229.1	240	242.1	119.7

5 Conclusions

The thermal, electrical, optical, and modulation properties are analyzed for the 980 nm InGaAs ICOC VCSELs with different structures of active layer.

Results show inserting quantum wells in maxima of the generated field increases the slope efficiency of L–I characteristic due to more efficient overlap the optical wave in the resonator and active layer, and reducing the current crowding.

The analysis of DC and modulation characteristics clarify that devices with 2 × 4 QWs have the largest slope efficiency of L–I characteristics and the widest modulation bandwidth. The modulation conversion efficiency factor is approximately 242 GHz/(A)$^{0.5}$ due to more efficient position of QWs in the resonator is presented.

Acknowlegments This work is supported by School of Photonic Science and Technology and BK21 in Korea.

References

Chu, K.-M., Lee, J.-S., Chu, K.-M., Cho, H.-S., Park, H.-H., Jeon, D.-Y.: A fluxless flip-chip bonding for VCSEL arrays using silver-coated indium solder bumps. IEEE Trans. Electron. Packag. Manuf. **27**, 246–250 (2004)

Hadley, G.R., Botez, D., Mawst, L.I.: Modal discrimination in leaky-mode (antiguided) arrays [diode lasers]. IEEE J. Quantum. Electron. **27**, 921–930 (1991)

Katz, J., Margalit, S., Harder, C., Wilt, D., Yariv, A.: The intrinsic electrical equivalent circuit of a laser diode. IEEE J. Quantum. Electron. **17**, 4–7 (1981)

Kim, J.K., Hall, E., Sjolund, O., Almuneau, G., Coldren, L.A.: Room temperature, electrically-pumped multiple-active-region VCSEL's with high differential efficiency at 1.55 mkm. Electron. Lett. **35**, 1085 (1999)

Krishnamoorthy, A.V., Chirovsky, L.M.F., Hobson, W.S., Lopata, J., Shah, J., Rozier, R., Cunningham, J.E., D'Asaro, L.A.: Small-signal characteristics of bottom-emitting intracavity contacted VCSEL's. IEEE Photon. Technol. Lett. **12**, 609–611 (2000)

Lear, K.L., Chalmers, S.A.: High single mode power conversion efficiency vertical cavity top surface emmiting lasers. IEEE Photon. Technol. Lett. **5**, 972–974 (1993)
Lysak, V.V., Chang, K.S., Lee, Y.T.: Current crowding in graded contact layers of intracavity-contacted oxide-confinement vertical-cavity surface-emitting lasers. Appl. Phys. Lett. **87**, 231118 (2005)
Lysak, V.V., Chang, K.S., Lee, Y.T.: Top mirror optimization of high-speed intracavity-contacted oxide confinement vertical-cavity surface-emitting lasers. J. Optoelectron. Adv. Mater. **8**, 355–358 (2006)
MacDougal, M.H., Geske, J., Lin, C.-K., Bond, A.E., Dapkus, P.D.: Low resistance intracavity contacted oxide-aperture VCSEL's. IEEE Photon. Technol. Lett. **10**, 9–11 (1998)
Nakwaski, W.: Thermal conductivity of binary, ternary, and quaternary III-V compounds. J. Appl. Phys. **64**, 159–166 (1988)
PICS3D, User's manual and reference manual, version 2002.2, Crosslight Inc., 2002
Piprek, J.: Semiconductor optoelectronics devices. Introduction to physics and simulation. pp. 279. Academic Press, Amsterdam (2003)
Raja, M.Y.A., Brueck, S.R.J., Osinski, M., Raja, C.F., Schaus, M.Y.A., McInerney, J.G., Brennan, T.M., Hammons, B.E.: Surface-emitting, multiple quantum well GaAs/AlGaAs laser with wavelength-resonant periodic gain medium. Appl. Phys. Lett. **53**, 1678–1680 (1988)
Sarzala, R.P., Nakwaski, W., Osinski, M.: Comprehensive thermal-electrical self-consistent model of proton-implanted top-surface-emitting lasers'. Int. J. Optoelectron. **10**, 357–371 (1996)
Sarzala, R.P.: Modelling of the threshold operation of 1.3-mkm GaAs-based oxide-confined (InGa)As/GaAs quantum-dot vertical-cavity surface-emitting lasers. IEEE J. Quantum. Electron. **40**, 629–639 (2004)
Scott, J.W., Geels, R.S., Corzine, S.W., Coldren, L.A.: Modeling temperature effects and spatial hole burning to optimize vertical-cavity surface-emitting laser performance. IEEE J. Quantum. Electron. **29**, 1295–1308 (1993)
Scott, J.W., Thibeault, B.J., Young, D.B., Coldren, L.A., Peters, F.H.: High efficiency submilliamp vertical cavity lasers with intracavity contacts. IEEE Photon. Technol. Lett. **6**, 678–680 (1994)
Sukhoivanov, I.A.: Influence of gain saturation and carrier dynamic models on the modulation response of quantum well lasers. Opt. Quantum. Electron. **31**, 1007 (1999)
Wilmsen, C., Temkin, H., Coldren, L.A. (eds.): Vertical cavity surface emitting lasers: design, fabrication, characterization, and application. pp. 455. Cambridge University Press, Cambridge (2003)
Wachutka, G.R.: Rigorous thermodynamic treatment of heat generation and conduction in semiconductor device modeling. IEEE Trans. Comput. Aided Des. **9**, 1141–1149 (1990)